

Electronic supplementary information

Sulfur-doped covalent triazine-based frameworks for enhanced photocatalytic hydrogen evolution from water under visible light

Liuyi Li,^{a, c} Wei Fang,^b Peng Zhang,^b Jinhong Bi,^{*a, b} Yunhui He,^a Jinyun Wang,^c and Wenyue Su^{*a}

^a *State Key Laboratory of Photocatalysis on Energy and Environment, Fuzhou University, Fuzhou 350002, P. R. China*

**E-mail: bijinhong@fzu.edu.cn; suweny@fzu.edu.cn*

^b *Department of Environmental Science and Engineering, Fuzhou University, Minhou, Fujian 350108, P. R. China*

^c *State Key Laboratory of Structural Chemistry, Fujian Institute of Research on the Structure of Matter, Chinese Academy of Sciences, Fuzhou, Fujian 350002, P. R. China*

Experimental Section

Materials: CTF-T1¹ and g-C₃N₄² was prepared by the previous reported method. Trifluoromethanesulfonic acid (99%) and terephthalonitrile (98%) were purchased from Adamas-beta. Sublimed sulfur (99.5%), dichloromethane, ammonia solution (25-28 vol%) and methanol were purchased from Sinopharm Chemical Reagent Co., Ltd. All reagents were directly used as received without further purification.

Synthesis of sulfur-doped CTF-T1: CTF-T1 (0.4 g) was mixed with 5wt% (0.02 g), 10wt% (0.04 g), 20wt% (0.08 g) and 30wt% (0.12 g) sublimed sulfur and well ground in an agate, respectively. Then the mixture was transfer into a quartz crucible and heated at 250 °C for 1 h with a ramping rate of 5 °C/min under flowing nitrogen gas. After cooling naturally, the solid product was milled into powder and refluxed by a Soxhlet extractor using methanol, then dried in air at 60 °C for 12 h. Finally, the resultant samples with different amount of sulfur were obtained and denoted as CTFS₅, CTFS₁₀, CTFS₂₀, CTFS₃₀, respectively. For comparison, the sample obtained by heating CTF without sublimed sulfur at the same reaction condition was denoted as CTFS₀. And the whole sulfur-doped CTFs were denoted as CTFS_x (x = 0, 5, 10, 20, 30).

Characterizations: Powder X-ray diffraction (PXRD) patterns of the as-prepared samples were collected on a Rigaku MiniFlex 600 X-ray diffractometer at 40 kV and 15 mA with Ni-filtered Cu K α irradiation (λ = 1.5406 Å). Fourier transform infrared (FTIR) spectra of the samples were obtained with a Thermo Scientific Nicolet iS10 spectrometer by using KBr pellets. The Brunauer-Emmett-Teller (BET) surface area was measured with an ASAP2020M apparatus (Micromeritics Instrument Corp.). X-ray photoelectron spectroscopy (XPS) measurements were performed on a PHI Quantum 2000 XPS system. All binding energies were referenced to the C1s peak (284.6 eV)

of the surface adventitious carbon. Solid-state UV-vis diffuse reflectance spectra (UV-vis DRS) were recorded at room temperature with a UV-vis spectrophotometer (Varian Cary 500) by using powder samples. Barium sulfate was used as a referent. The photoluminescence (PL) spectra were measured by an Edinburgh FL/FS900 spectrophotometer with an excitation wavelength at 360 nm. The scanning electron microscopy (SEM) images were obtained with a Nova NanoSEM 230 microscopy (FEI Corp.). The transmission electron microscopy (TEM) data were recorded using a JEOL model JEM 2010 EX microscope at an accelerating voltage of 200 kV. Thermogravimetry analysis (TGA) was carried out on a NETZSCH Simultaneous Thermal Analyzer (STA 449C). A 300 W Xe lamp (PLS-SXE300C) with a 420 nm cut-off filter was used as light source.

Photoelectrochemical measurement: To fabricate the working electrode, 5 mg of fully ground sample and 0.5 mL of N,N-dimethylformamide (DMF) were mixed under sonication for 30 min to make them fully dispersible. 10 μ L of the obtained slurry was dropped onto a piece of fluoride-tin oxide (FTO) glass substrates with a cover area of 0.25 cm². The uncovered parts of the electrode were coated with epoxy. Then the working electrode was obtained after drying in air naturally. The photocurrents were recorded by an electrochemical workstation (CHI650E) equipped with a conventional three-electrode cell. A platinum plate electrode and an Ag/AgCl electrode were used as the counter electrode and the reference electrode, respectively. The electrodes were immersed in a 0.2 M Na₂SO₄ aqueous solution for 30 s before measurement. The working electrode was illuminated by a 300 W Xe lamp (PLS-SXE300C) with a 420 nm cut-off filter from the backside to minimize the impact of thickness of the semiconductor layer. Each measurement was repeated three times under ambient conditions.

Photocatalytic activity evaluation: Photocatalytic hydrogen evolution from water-splitting

reaction was carried out with powder samples to provide sufficient surface area in a glass-closed gas-circulation system and a 100 mL Pyrex glass reaction vessel. The reaction was performed by dispersing 20 mg of catalyst into an aqueous solution (50 mL) containing triethanolamine (10 vol %) as a sacrificial electron donor. An amount of $\text{H}_2\text{PtCl}_6 \cdot 6\text{H}_2\text{O}$ was dissolved in the reactant solution to deposit 1 wt% of Pt onto the surface of catalyst by the in situ photodeposition method. The whole reaction system was evacuated to completely remove air before irradiating under visible light which was controlled by a 420 nm cut-off filter. The temperature of the reactant solution was kept at a constant temperature by a flow of cooling water during the reaction. The amount of H_2 evolution was analyzed by using an on-line gas chromatograph (SHIMADZU, GC-8A) with a thermal conductivity detector (TCD) and using Argon as the carrier gas. To evaluate the stability of the photocatalyst, the photocatalytic reactions were carried out as the similar procedure above by 40 mg catalyst for a total of 16 h with evacuation every 4 h.

Theoretical Calculations

To understand the electron properties of the investigated compounds **CTF-T1-MC** and **CTFS-MC**, the density functional theory (DFT) method at the hybrid Becke three-parameter Lee-Yang-Parr (B3LYP)³ functional level was used to optimize the geometrical structures firstly. During the optimization processes, the convergent values of maximum force, root-mean-square (RMS) force, maximum displacement, and RMS displacement were set by default. Then, the natural bond orbital (NBO) analysis⁴ was implemented. In these calculations, the all-electron basis set of 6-311G**⁵ was used. All calculations were implemented in Gaussian 09 program.⁶ Visualization of the optimized geometrical structures, frontier molecular orbitals, and electrostatic potential (ESP) mapped onto electron density surfaces were performed by GaussView.

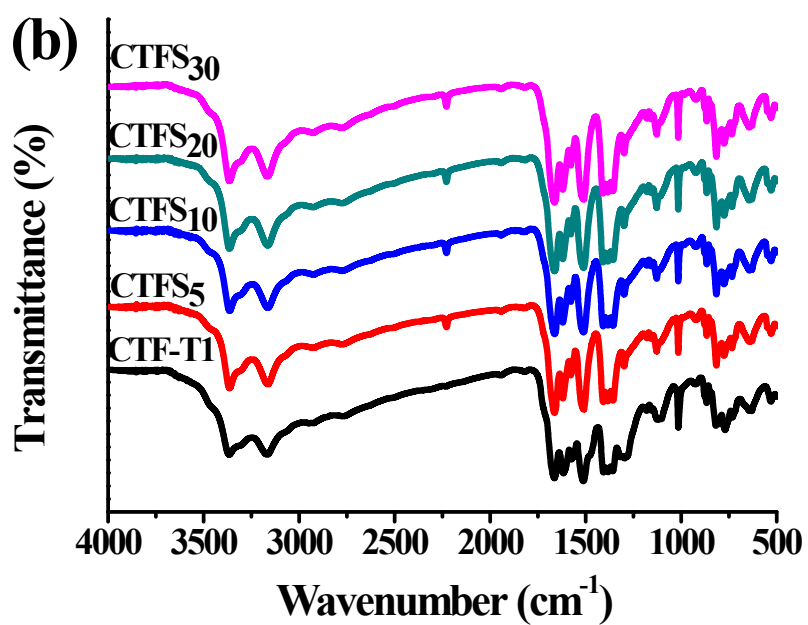
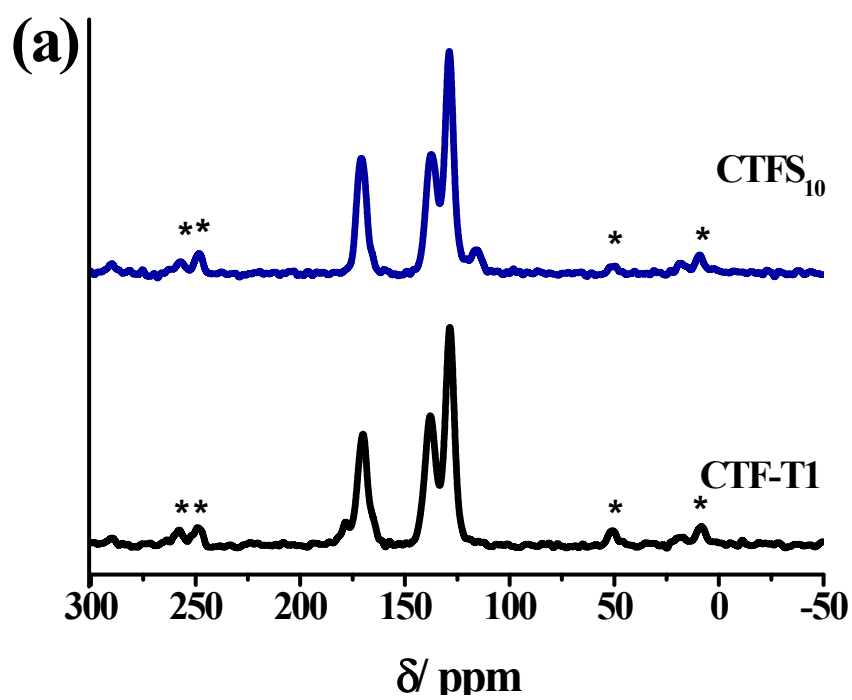


Figure S1. Solid state ¹³ CNMR (a) of CTF-T1 and CTFS₁₀, FTIR (b) of CTF-T1 and CTFS_x.

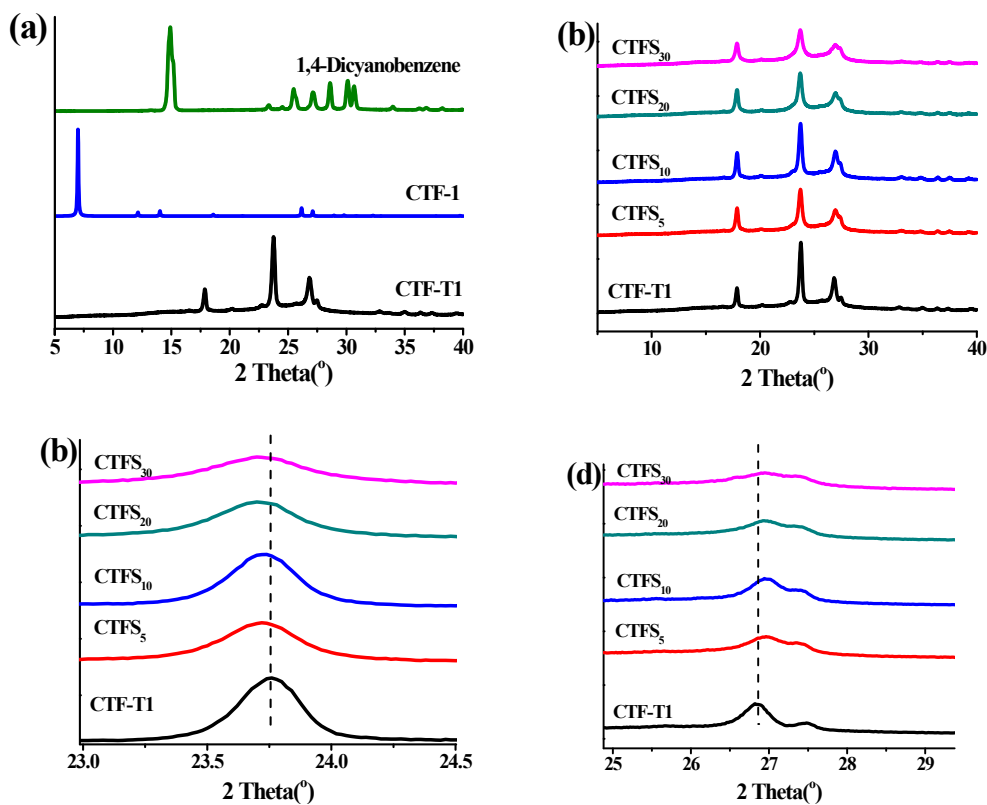


Figure S2. PXRD patterns of CTF-1, CTF-T1 and 1,4-dicyanobenzene (a), CTF-T1 and CTFS_x (b) and high magnification of CTF-T1 and CTFS₁₀ (c, d).

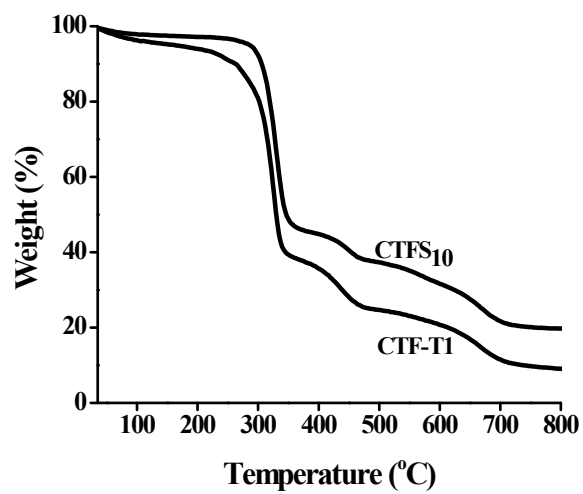


Figure S3. TGA curves of CTF-T1 and CTFS₁₀.



Figure S4. SEM images of CTF-T1

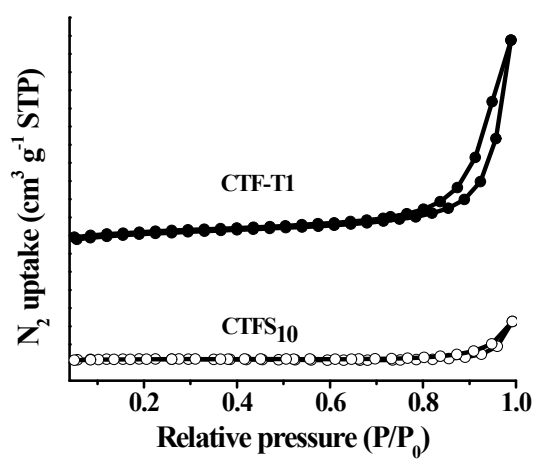


Figure S5. N_2 adsorption-desorption isotherms of CTF-T1 and CTFS₁₀

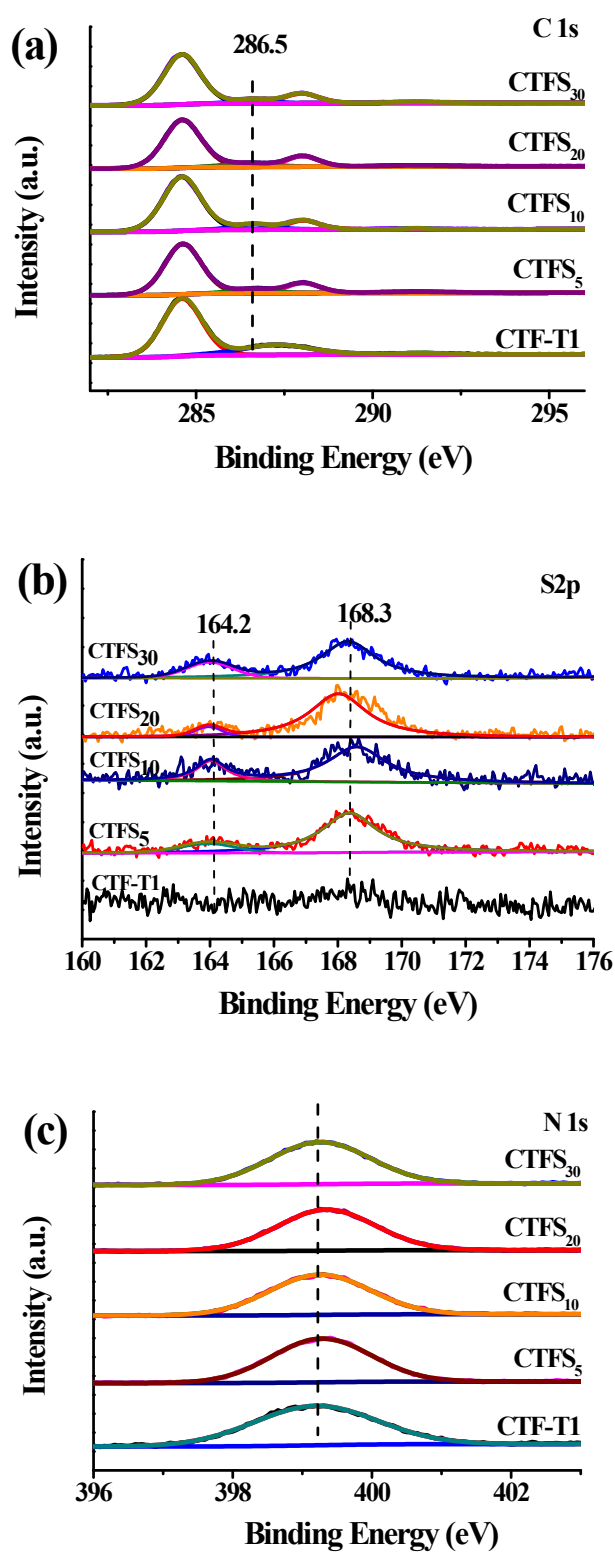


Figure S6. XPS spectra of C1s (a), S2p (b) and N1s (c) for CTF-T1 and CTFS_x.

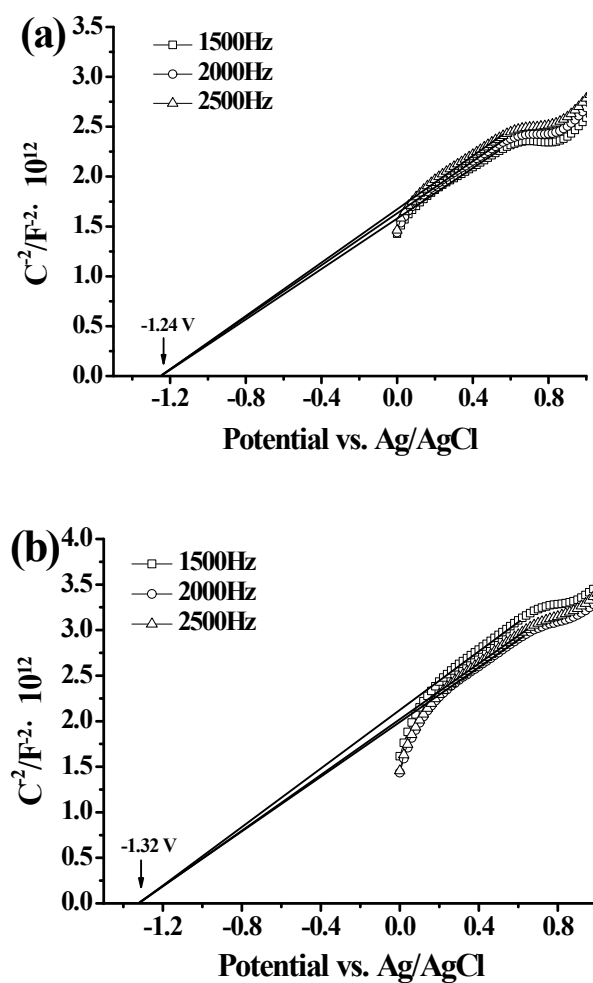


Figure S7. Mott-Schottky plots of of CTF-T1 (a) and CTFS₁₀ (b). The MS plots were obtained at a frequency of 1 kHz in an aqueous solution of Na₂SO₄(0.1 M).

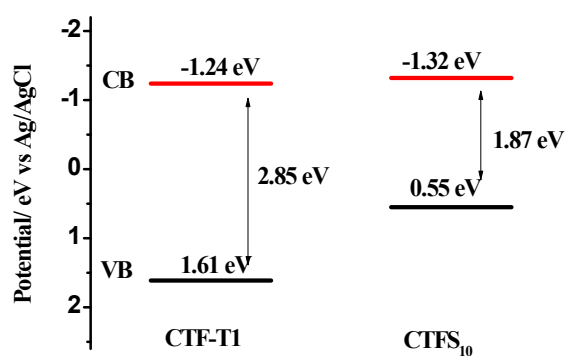


Figure S8. Electronic band structure of CTF-T1 and CTFS₁₀.

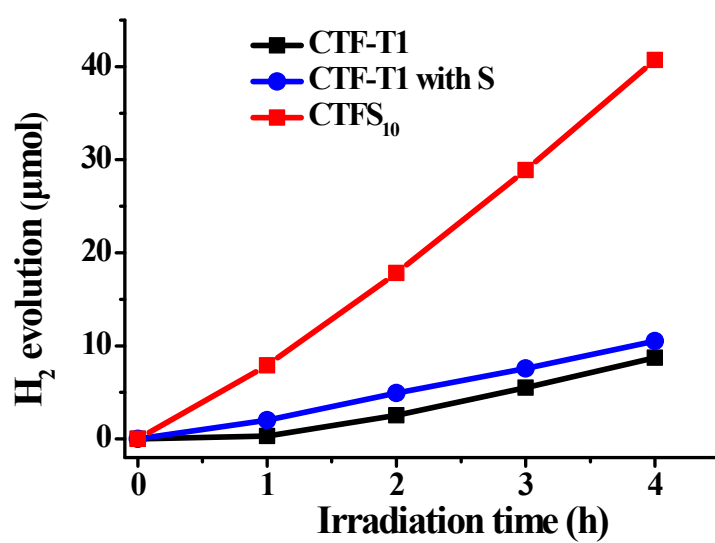


Figure S9. Hydrogen evolution rates of CTF-T1, CTFS₁₀ and CTF-T1 with S.

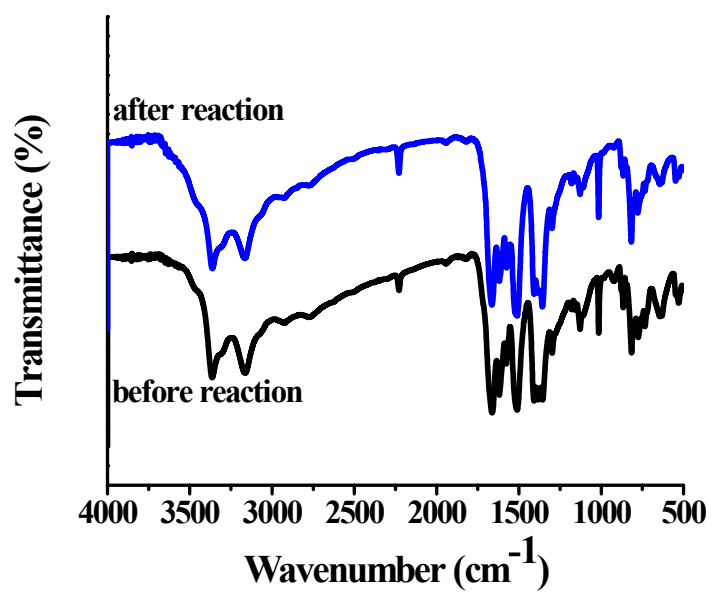


Figure S10. IR spectra of CTFS₁₀.before and after catalytic reaction.

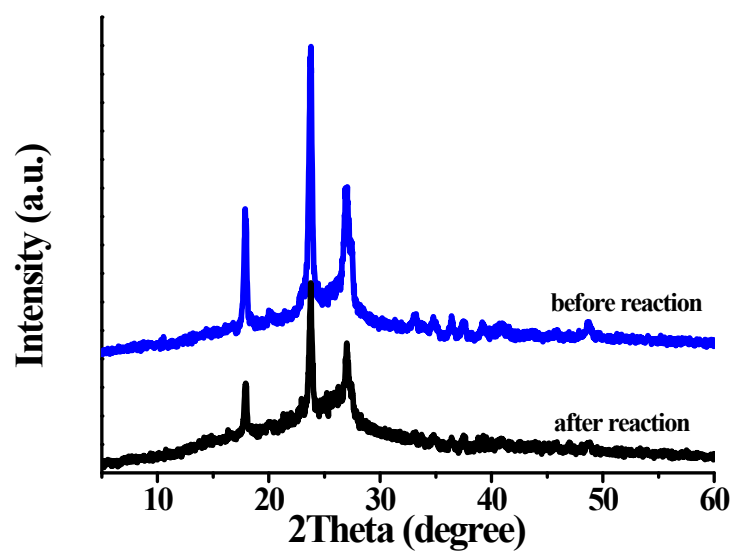


Figure S11. PXRD patterns of CTFS₁₀.before and after catalytic reaction.

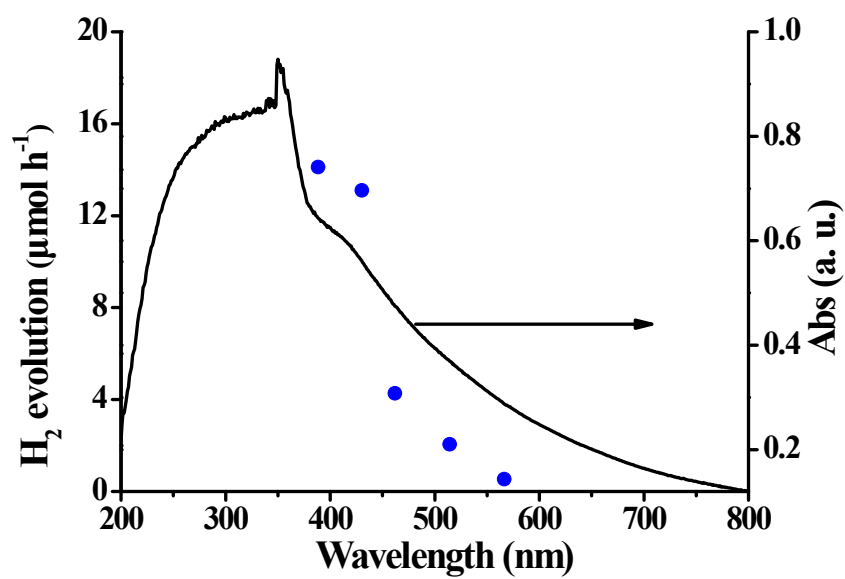


Figure S12. Wavelength-dependent H₂ evolution from water by CTFS₁₀.

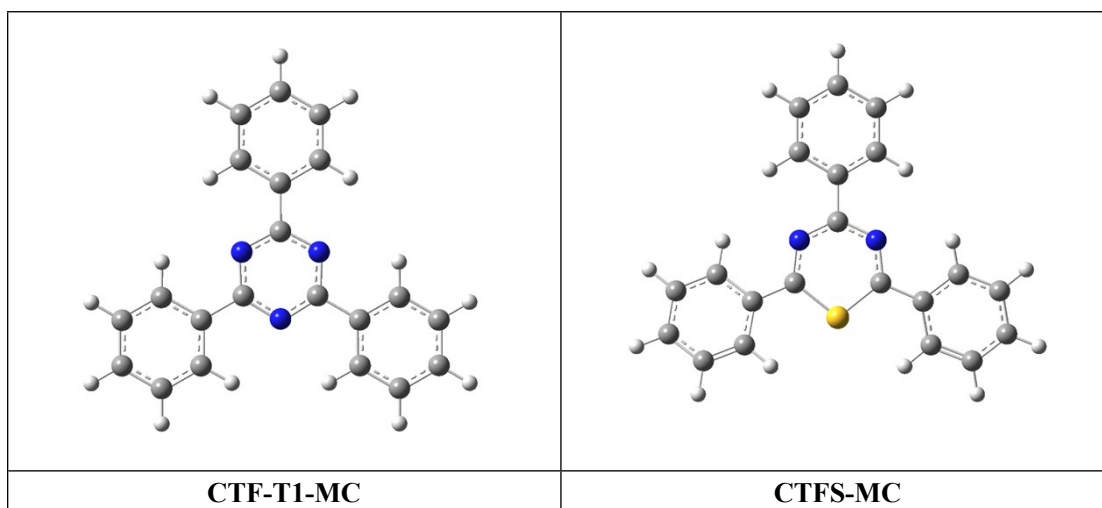


Figure S13. The optimized structures of investigated compounds **CTF-T1-MC** and **CTFS-MC** by DFT method at the B3LYP level. The yellow, blue, gray, and white spheres represent sulfur, nitrogen, carbon, and hydrogen atoms, respectively.

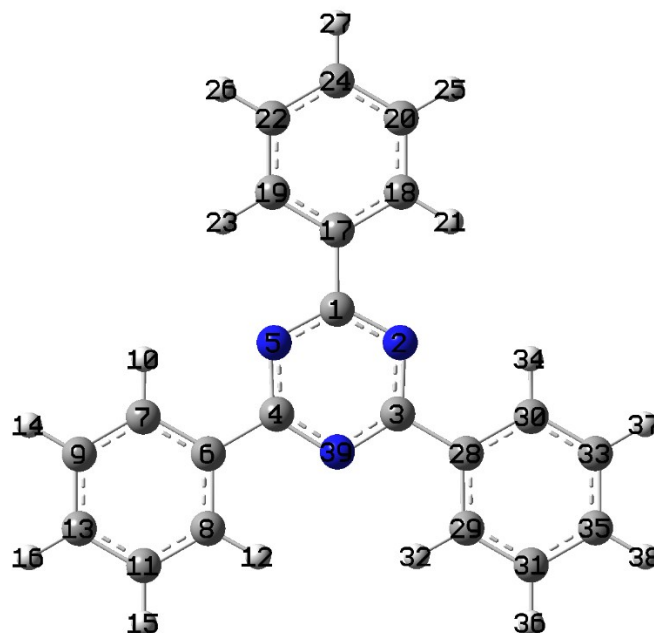


Table S1 The Optimized Geometrical Coordinates (unit: angstroms) and Natural Population Analysis (NPA) (unit: electron) of Compound **CTF-T1-MC** by DFT Method at the B3LYP Level.

center number	atomic type	Charge	coordinates		
			X	Y	Z
1	C	0.506	0.80	1.04	0.00
2	N	-0.554	1.35	-0.18	0.00
3	C	0.505	0.50	-1.21	0.00
4	C	0.505	-1.30	0.17	0.00
5	N	-0.554	-0.52	1.26	0.00
6	C	-0.099	-2.77	0.36	0.00
7	C	-0.169	-3.32	1.65	0.00
8	C	-0.167	-3.63	-0.74	0.00
9	C	-0.199	-4.70	1.83	0.00
10	H	0.227	-2.65	2.50	0.00
11	C	-0.199	-5.01	-0.56	0.00
12	H	0.226	-3.20	-1.74	0.00
13	C	-0.183	-5.55	0.72	0.00
14	H	0.206	-5.11	2.83	0.00
15	H	0.206	-5.67	-1.43	0.00
16	H	0.204	-6.62	0.86	0.00
17	C	-0.092	1.70	2.22	0.00
18	C	-0.171	3.09	2.05	0.00

19	C	-0.170	1.17	3.52	0.00
20	C	-0.199	3.93	3.15	0.00
21	H	0.225	3.49	1.04	0.00
22	C	-0.199	2.02	4.62	0.00
23	H	0.225	0.10	3.64	0.00
24	C	-0.185	3.40	4.44	0.00
25	H	0.205	5.01	3.01	0.00
26	H	0.205	1.60	5.62	0.00
27	H	0.204	4.06	5.30	0.00
28	C	-0.099	1.07	-2.58	0.00
29	C	-0.167	0.23	-3.70	0.00
30	C	-0.169	2.46	-2.77	0.00
31	C	-0.199	0.76	-4.98	0.00
32	H	0.226	-0.84	-3.54	0.00
33	C	-0.199	2.99	-4.06	0.00
34	H	0.227	3.11	-1.90	0.00
35	C	-0.183	2.15	-5.16	0.00
36	H	0.206	0.10	-5.84	0.00
37	H	0.206	4.07	-4.19	0.00
38	H	0.204	2.56	-6.17	0.00
39	N	-0.560	-0.83	-1.08	0.00

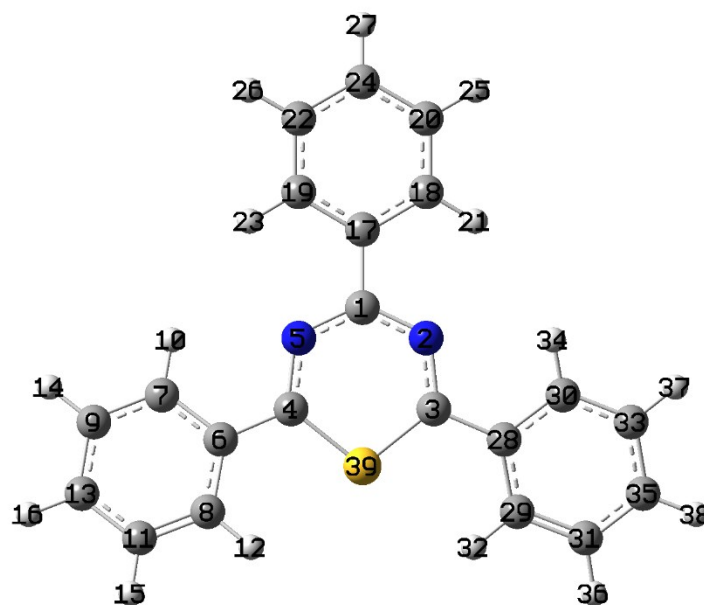


Table S2 The Optimized Geometrical Coordinates (unit: angstroms) and Natural Population Analysis (NPA) (unit: electron) of Compound **CTFS-MC** by DFT Method at the B3LYP Level.

center number	atomic type	Charge	coordinates		
			X	Y	Z
1	C	0.506	0.00	-1.21	0.00
2	N	-0.548	-1.20	-0.64	0.08
3	C	-0.183	-1.35	0.71	0.02
4	C	-0.183	1.35	0.71	-0.02
5	N	-0.548	1.20	-0.64	-0.08
6	C	-0.037	2.68	1.29	0.00
7	C	-0.194	3.79	0.45	-0.23
8	C	-0.213	2.93	2.66	0.26
9	C	-0.188	5.08	0.96	-0.22
10	H	0.229	3.61	-0.60	-0.42
11	C	-0.192	4.22	3.16	0.26
12	H	0.206	2.11	3.33	0.47
13	C	-0.203	5.31	2.31	0.03
14	H	0.205	5.92	0.29	-0.40
15	H	0.205	4.38	4.21	0.46
16	H	0.204	6.32	2.71	0.04
17	C	-0.092	0.00	-2.70	0.00
18	C	-0.169	-1.21	-3.41	-0.06
19	C	-0.169	1.21	-3.41	0.06
20	C	-0.202	-1.21	-4.80	-0.06

21	H	0.226	-2.13	-2.85	-0.11
22	C	-0.202	1.21	-4.80	0.06
23	H	0.226	2.13	-2.85	0.11
24	C	-0.185	0.00	-5.50	0.00
25	H	0.204	-2.14	-5.34	-0.11
26	H	0.204	2.14	-5.34	0.11
27	H	0.203	0.00	-6.58	0.00
28	C	-0.037	-2.68	1.29	0.00
29	C	-0.213	-2.93	2.66	-0.26
30	C	-0.194	-3.79	0.44	0.23
31	C	-0.192	-4.22	3.16	-0.26
32	H	0.206	-2.11	3.33	-0.46
33	C	-0.188	-5.08	0.96	0.22
34	H	0.229	-3.61	-0.60	0.42
35	C	-0.203	-5.31	2.31	-0.03
36	H	0.205	-4.38	4.21	-0.46
37	H	0.205	-5.92	0.29	0.40
38	H	0.204	-6.32	2.71	-0.03
39	S	0.867	0.00	1.79	0.00

References

- 1 J. Bi, W. Fang, L. Li, J. Wang, S. Liang, Y. He, M. Liu and L. Wu, *Macromol. Rapid Commun.*, 2015, **36**, 1799.
- 2 X. Wang, K. Maeda, A. Thomas, K. Takanabe, G. Xin, J. M. Carlsson, K. Domen and M. Antonietti, *Nat. Mater.*, 2009, **8**, 76.
- 3 (a) Lee, C. T.; Yang, W. T.; Parr, R. G. *Phys. Rev. B* **1988**, *37*, 785-789; (b) Becke, A. D. *J. Chem. Phys.* **1993**, *98*, 5648.
2. (a) Reed, A. E.; Weinhold, F. *J. Chem. Phys.* **1983**, *78*, 4066; (b) Reed, A. E.; Weinstock, R. B.; Weinhold, F. *J. Chem. Phys.* **1985**, *83*, 735; (c) Reed, A. E.; Curtiss, L. A.; Weinhold, F. *Chem. Rev.* **1988**, *88*, 899.
3. Francl, M. M.; Pietro, W. J.; Hehre, W. J.; Binkley, J. S.; Gordon, M. S.; DeFrees, D. J.; Pople, J. A. *J. Chem. Phys.* **1982**, *77*, 3654.

4. Frisch, M. J.; Trucks, G. W.; Schlegel, H. B.; Scuseria, G. E.; Robb, M. A.; Cheeseman, J. R.; Scalmani, G.; Barone, V.; Mennucci, B.; Petersson, G. A.; Nakatsuji, H.; Caricato, M.; Li, X.; Hratchian, H. P.; Izmaylov, A. F.; Bloino, J.; Zheng, G.; Sonnenberg, J. L.; Hada, M.; Ehara, M.; Toyota, K.; Fukuda, R.; Hasegawa, J.; Ishida, M.; Nakajima, T.; Honda, Y.; Kitao, O.; Nakai, H.; Vreven, T.; Montgomery, J. A., Jr.; Peralta, J. E.; Ogliaro, F.; Bearpark, M.; Heyd, J. J.; Brothers, E.; Kudin, K. N.; Staroverov, V. N.; Keith, T.; Kobayashi, R.; Normand, J.; Raghavachari, K.; Rendell, A.; Burant, J. C.; Iyengar, S. S.; Tomasi, J.; Cossi, M.; Rega, N.; Millam, J. M.; Klene, M.; Knox, J. E.; Cross, J. B.; Bakken, V.; Adamo, C.; Jaramillo, J.; Gomperts, R.; Stratmann, R. E.; Yazyev, O.; Austin, A. J.; Cammi, R.; Pomelli, C.; Ochterski, J. W.; Martin, R. L.; Morokuma, K.; Zakrzewski, V. G.; Voth, G. A.; Salvador, P.; Dannenberg, J. J.; Dapprich, S.; Daniels, A. D.; Farkas, O.; Foresman, J. B.; Ortiz, J. V.; Cioslowski, J.; Fox, D. J. *Gaussian 09, revision D.01*. Gaussian, Inc., Wallingford CT, 2013.